Black hole immersed dark matter halo

Zhaoyi Xu,[1,*] Xiaobo Gong,[2,3,5,†] and Shuang-Nan Zhang[1,3,4,‡]

[1]*Key Laboratory of Particle Astrophysics, Institute of High Energy Physics, Chinese Academy of Sciences, Beijing 100049, China*

[2]*Yunnan Observatories, Chinese Academy of Sciences, 396 Yangfangwang, Guandu District, Kunming, 650216, China*

[3]*University of Chinese Academy of Sciences, Beijing 100049, China*

[4]*National Astronomical Observatories of China, Chinese Academy of Sciences, Beijing 100012, China*

[5]*Key Laboratory for the Structure and Evolution of Celestial Objects, Chinese Academy of Sciences, 396 Yangfangwang, Guandu District, Kunming 650216, China*

(Received 2 July 2019; revised manuscript received 4 December 2019; published 9 January 2020)

In this work, based on the constant for the equation of state ω, we obtain the Schwarzschild-like black hole solutions in some dark matter halos. We also generalize these black hole metrics to Kerr-like black hole solutions with Newman-Janis algorithm. For an example, we derive the specific black hole space-time metrics in the case of the cold dark matter halo and Bose-Einstein condensation dark matter halo. Following the above two black hole metrics, we discuss how a dark matter halo changes the properties of black holes, including the event horizon structure (these results agree with that obtained by Liu and Zhang [Phys. Lett. B **679**, 88 (2009).] in the case of gravitational collapse), stationary limit surfaces, ergosphere, and singularity structure. Our results may help us understand the interaction between the dark matter halo and supermassive black holes at the centers of galaxies.

DOI: 10.1103/PhysRevD.101.024029

I. INTRODUCTION

Astronomical observations show that the matter composition of our Universe consists mainly of 4.9% baryon matter, 26.8% dark matter, and 68.3% dark energy [1]. For galaxies, the effects of dark matter are extremely important. Here, we introduce the dark matter model and its problems [2,3]. Because of the rotation curves of galaxies, the mass-light ratio of elliptical galaxies, the cosmic microwave background radiation, and the large-scale structure of the Universe, a lot of research has been done on dark matter and proposed various dark matter models, such as the cold dark matter (CDM) model [4,5], warm dark matter model [6,7], self-interacting dark matter model [8], Bose-Einstein condensation (BEC) dark matter (DM) model [9–12], modified Newtonian dynamic model [13], and superfluid dark matter model [14]. Astronomers are concerned with the spatial density distribution of dark matter. On a large scale (for example, the outer edges of galaxies and clusters of galaxies), the spatial density distribution of this dark matter has been well understood [1], but the spatial density distribution of dark matter is not clear when it is close a supermassive black hole (SMBH) or the central part of the galaxy [3]. Therefore, how dark matter is distributed near the black hole becomes an interesting and important problem. It is generally believed that, due to the existence of black holes, the spike phenomenon occurs in the distribution of dark matter near the black hole [15,16].

On the other hand, the existence of black holes is widely established [17–20], due to the observation of the orbital motion of the S-stars in the center of the Milky Way [21–23], the observations of Laser Interferometer Gravitational Wave Observatory on gravitational waves, and the study of active galactic nuclei. Recently, the Event Horizon Telescope observed the black hole shadow in M87, which further confirms the existence of black holes [24]. Because there is a lot of dark matter around the black hole at the center of the galaxy, how dark matter changes the black hole space-time is an interesting problem. So far, this issue has been studied from the following aspects. First, in the early time of black hole formation, dark matter makes black holes grow faster and makes it easier to form SMBHs in the early Universe [25–28]. On the other hand, Refs. [29,30] (and many references therein) do offer other density profiles consistent with rapid black hole growth in the nonrelativistic case. Second, the presence of dark matter changes the space-time structure of black holes in principle, but there are still some problems in these studies. One of the most important issues is how to solve the Einstein's field equation when considering the dark matter background. In fact, in the case of gravitational collapse, Ref. [31] found

*xuzy@ihep.ac.cn
†zhangsn@ihep.ac.cn
‡xbgong@ynao.ac.cn

that the distribution of external matter changes the internal metric. For example, the external matter causes the event horizon of the black hole to expand. But they did not get the external matter to change the metric of the Kerr black hole. At the same time, they did not consider the more general matter distribution case such as dark matter distribution. Recently, Ref. [32] did some work in this area, but it only considered the special case of $f(r) = g(r)$, where $f(r)$ and $g(r)$ are metric coefficients. In fact, when considering the dark matter halo, $f(r) \neq g(r)$, and we still do not know how dark matter changes the space-time structure of black holes. In this work, we develop an asymptotic expansion method to study this problem.

The structure of the article is as follows. In Sec. II, we introduce the dark matter density distributions. In Sec. III, by solving the Einstein's field equation, we obtain the Schwarzschild-like black hole solutions in the dark matter halos. In Sec. IV, through the Newman-Janis (NJ) algorithm, we obtain a Kerr-like black hole solution in the dark matter halo. In Sec. V, we discuss the event horizons, stationary limit surfaces, ergospheres, and singularities of these black holes. The summary is in Sec. VI.

II. DARK MATTER DENSITY PROFILE

A. CDM and NFW profile

At the galaxy scale, the behavior of dark matter is mainly reflected in the density distribution. For the CDM model, the corresponding distribution is the Navarro-Frenk-White (NFW) profile [4,5]. This density profile is derived from a numerical simulation based on the ΛCDM model (Λ is the cosmological constant), and its mathematical expression is

$$\rho_{\mathrm{NFW}} = \frac{\rho_s}{\frac{r}{R_s}(1+\frac{r}{R_s})^2}, \tag{1}$$

where ρ_s is the critical density and R_s is the scale radius. From the NFW profile [Eq. (1)], we can learn that when r approaches to 0 the dark matter density tends to infinity. This is the so-called cusp phenomenon [3,33].

B. BEC DM and Thomas-Fermi profile

For the BEC DM model, the dark matter density distribution becomes more interesting [9–12,34]. In this model, when the scale is large (such as outside the galaxy, galaxy group, and Universe), the behavior of dark matter is consistent with the CDM model. But when r approaches to 0, the dark matter density approaches to constant. For the BEC DM model, the dark matter density profile [Thomas-Fermi (TF) approximation] is

$$\rho_{\mathrm{TF}} = \rho_s \frac{\sin(kr)}{kr}, \tag{2}$$

where $k = \sqrt{Gm^3/\hbar^2 a} = \pi/R$, ρ_s is the center density of BEC DM and R is the radius when the dark matter pressure and density are zero. m is mass of the ultralight particle, and a is the Compton scattering length.

III. SCHWARZSCHILD-LIKE BLACK HOLE METRIC IN DARK MATTER HALO

For the case of a Schwarzschild-like black hole, the space-time metric can be expressed as

$$ds^2 = -f(r)dt^2 + \frac{1}{g(r)}dr^2 + r^2 d\Omega^2, \tag{3}$$

where $d\Omega^2 = d\theta^2 + \sin^2\theta d\phi^2$ and $f(r)$ and $g(r)$ are space-time coefficients. For the convenience of calculation, we rewrite them as

$$f(r) = e^{2\Phi(r)} \tag{4}$$

and

$$g(r) = 1 - \frac{B(r)}{r}, \tag{5}$$

where $\Phi(r)$ and $B(r)$ are the functions of r, which are determined by Einstein's field equation and the equation of state. We all know that when we do not consider dark matter the above black hole solution will degenerate into the Schwarzschild solution; then, $\Phi(r) = \ln(1-2M/r)$ and $B(r) = 2M$, where M is the black hole mass.

For a general dark matter density distribution, the energy-momentum tensor can be written as $T_{\mu\nu} = \mathrm{diag}(-\rho, P_r, P_\theta, P_\phi)$. Under these simplifications, Einstein's field equation $G_{\mu\nu} = 8\pi T_{\mu\nu}$ will become the following form:

$$8\pi\rho(r) = \frac{B'(r)}{r^2}, \tag{6}$$

$$8\pi P_r(r) = -\frac{B(r)}{r^3} + 2\left(1-\frac{B(r)}{r}\right)\frac{\Phi'(r)}{r}, \tag{7}$$

$$\begin{aligned} 8\pi P_\theta(r) &= 8\pi P_\phi(r) \\ &= \left(1-\frac{B(r)}{r}\right)\left[\Phi''(r) + \Phi'^2(r) \right. \\ &\quad - \frac{rB'(r)-B(r)}{2r(r-B(r))}\Phi'(r) \\ &\quad \left. - \frac{rB'(r)-B(r)}{2r^2(r-B(r))} + \frac{\Phi'(r)}{r}\right]. \end{aligned} \tag{8}$$

To solve the above equations, we need to know the equation of state, which is the relationship between density and pressure. In this work, we use the equation of state $P_r(r) = \omega(r)\rho(r)$, where $\omega(r)$ is the function of r. For a

general case, due to the requirement of the asymptotic expansion method, $\omega(r)$ will satisfy a certain condition. But for the sake of simplicity, we only consider the constant case. Through energy-momentum tensor conversation law $T^{\mu\nu}_{;\nu}=0$, we get the following equation:

$$P_r' = -(P_r+\rho)\Phi' + \frac{2(P_\theta - P_r)}{r}. \tag{9}$$

This equation can be understood as a relativistic Euler equation. If we consider the isotropic pressure $P_\theta = P_r$, we can get a lot of black hole solutions. In our study, we do not think about this case. On the other hand, combining the equation of state $\omega(r)$ and the gravitational field equation [Eqs. (6) and (7)], we obtain

$$\Phi'(r) = \frac{B(r)}{2r^2(1-B(r)/r)} + \omega(r)\frac{rB'(r)}{2r^2(1-B(r)/r)}. \tag{10}$$

If the dark matter density is not considered, the black hole solution degenerates to the Schwarzschild black hole ($\rho_s = 0$). For the dark matter case, we are going to use the following steps to get the black hole solution. First, substituting the dark matter density distribution into Eq. (6), we get the function $B(r)$. Second, substituting $B(r)$ into Eq. (10), we obtain $\Phi'(r)$. To get an analytic expression of $\Phi(r)$, we have to deal with a complicated integral. Here, we use asymptotic expansion to obtain the analytic expression of $\Phi(r)$. In this work, we consider a general dark matter distribution near the black hole, and this distribution satisfies the following condition: when r tends to infinity, the dark matter density $\rho(r) \to 0$. As far as we know, all dark matter distributions satisfy this condition. For the sake of convenience, we set $B(r) = 2M + K(r)$. The asymptotic form of the function $\Phi'(r)$ is analyzed by means of series expansion (which is in powers of $\frac{K(r)}{r-2M}$). The result is

$$\begin{aligned}
2\Phi'(r) &= \left(\frac{2M}{r^2} + \frac{K(r)+r\omega(r)K'(r)}{r^2}\right)\frac{1}{1-\frac{2M}{r}-\frac{K(r)}{r}} = \left(\frac{2M}{r^2} + \frac{K(r)+r\omega(r)K'(r)}{r^2}\right)\frac{\frac{r}{r-2M}}{1-\frac{K(r)}{r-2M}} \\
&= \left(\frac{2M}{r^2} + \frac{K(r)+r\omega(r)K'(r)}{r^2}\right)\frac{r}{r-2M}\left[1+\frac{K(r)}{r-2M}+\left(\frac{K(r)}{r-2M}\right)^2+\left(\frac{K(r)}{r-2M}\right)^3+o\left(\left(\frac{K(r)}{r-2M}\right)^3\right)\right] \\
&= \frac{2M}{r(r-2M)} + \frac{K+r\omega K'}{r(r-2M)} + \frac{K(2M+K+r\omega K')}{r(r-2M)^2} + \cdots.
\end{aligned} \tag{11}$$

The function $\omega(r)$ satisfies

$$K(r) + r\omega(r)K'(r) < r^2. \tag{12}$$

Where $X' = dX/dr$, the X can be $K(r)$, $\Phi(r)$, $B(r)$, or $P_r(r)$. From Eqs. (6) and (7), we find that if $\rho_s = 0$ then $2\Phi'(r) = 2M/(r(r-2M))$, $f(r) = e^{2\Phi} = 1 - 2M/r$. This is the Schwarzschild black hole solution.

Next, we calculate the Schwarzschild-like black hole solutions in dark matter halos, and these dark matter density profiles include the NFW profile and TF profile. From now on, we take the equation of state as a constant $\omega(r) = \omega$.

A. Case I NFW profile

For a CDM halo, from Eqs. (1), (6), and (11), we obtain

$$B(r) = 2M + K(r) = 2M + 8\pi\int r^2\rho_{\rm NFW}dr = 2M + 8\pi\rho_s R_s^3\left[\ln\left(1+\frac{r}{R_s}\right) + \frac{R_s}{r+R_s} - 1\right], \tag{13}$$

$$K(r) = 8\pi\rho_s R_s^3\left[\ln\left(1+\frac{r}{R_s}\right) + \frac{R_s}{r+R_s} - 1\right], \tag{14}$$

$$\begin{aligned}
f(r) = e^{2\Phi} = \left(1-\frac{2M}{r}\right) &\times r^{-\frac{4\pi\rho_s R_s^3}{M}} \times (r+R_s)^{-\frac{8\pi\rho_s R_s^3(\omega - R_s - 2M)}{(R_s+2M)^2}} \times (r-2M)^{\frac{8\pi\rho_s R_s^3(\omega+R_s+\frac{R_s^2}{2M})}{(R_s+2M)^2}} \times \mathrm{Exp}\left[\frac{8\pi\rho_s R_s^3\omega}{R_s+2M}\frac{1}{r+R_s} + \frac{4\pi\rho_s R_s^3}{M}\right. \\
&\left.\times\left[\ln\left(1+\frac{r}{R_s}\right)\times\ln\left(\frac{|r-2M|}{R_s+2M}\right) + \mathrm{PolyLog}\left(2,-\frac{r}{R_s}\right) + \mathrm{PolyLog}\left(2,\frac{r+R_s}{R_s+2M}\right)\right]\right],
\end{aligned} \tag{15}$$

where $\mathrm{PolyLog}(n,x)$ represents the polylogarithm function $\mathrm{Li}_n(x)$ of index n at the point x. Specifically, they are $\mathrm{PolyLog}(2,-r/R_s)=\sum_{k=1}^{\infty}\frac{1}{k^2}(-\frac{r}{R_s})^k$ and $\mathrm{PolyLog}(2,\frac{r+R_s}{R_s+2M})=\sum_{k=1}^{\infty}\frac{1}{k^2}(\frac{r+R_s}{R_s+2M})^k$. When $r\sim 0$, $\mathrm{PolyLog}(2,-r/R_s)\sim 0$; if $r\sim R_s$, the $\mathrm{PolyLog}(2,-r/R_s)\sim -\frac{\pi^2}{12}$; when $r\sim 2M$, then $\mathrm{PolyLog}(2,\frac{r+R_s}{R_s+2M})=\mathrm{PolyLog}(2,1)=\frac{\pi^2}{6}$.

B. Case II TF profile

For a BEC DM halo, from Eqs. (2), (6), and (11), we obtain

$$B(r)=2M+K(r)=2M+8\pi\int r^2\rho_{TF}dr=2M+\frac{8G\rho_sR^3}{\pi^2}\left[\sin\left(\frac{\pi r}{R}\right)-\frac{\pi r}{R}\cos\left(\frac{\pi r}{R}\right)\right], \tag{16}$$

$$K(r)=\frac{8G\rho_sR^3}{\pi^2}\left[\sin\left(\frac{\pi r}{R}\right)-\frac{\pi r}{R}\cos\left(\frac{\pi r}{R}\right)\right], \tag{17}$$

$$\begin{aligned}f(r)=e^{2\Phi}=&\left(1-\frac{2M}{r}\right)\times\mathrm{Exp}\left[\frac{8\rho_sR^2\omega}{\pi}\cos\left(\frac{\pi r}{R}\right)-\frac{1}{2M}\mathrm{Ci}\left[\frac{\pi}{R}(r-2M)\right]\times\left[-\frac{16MG\rho_sR^2}{\pi}\cos\left(\frac{2M\pi}{R}\right)\right.\right.\\&+8\rho_sR\left(\frac{GR^2}{\pi^2}+4M^2\omega\right)\sin\left(\frac{2M\pi}{R}\right)\left.\left.\right]+\frac{4G\rho_sR^3}{M\pi^2}\mathrm{Si}\left[\frac{\pi r}{R}\right]-\frac{4G\rho_sR^3}{M\pi^2}\cos\left(\frac{2M\pi}{R}\right)\mathrm{Si}\left[\frac{\pi}{R}(r-2M)\right]\right.\\&\left.-16M\rho_sR\omega\cos\left(\frac{2M\pi}{R}\right)\mathrm{Si}\left[\frac{\pi}{R}(r-2M)\right]-\frac{8G\rho_sR^2}{\pi}\sin\left(\frac{2M\pi}{R}\right)\mathrm{Si}\left[\frac{\pi}{R}(r-2M)\right]\right],\end{aligned} \tag{18}$$

where $\mathrm{Si}[x]=\int\frac{\sin(x)}{x}dx$ and $\mathrm{Ci}[x]=\int\frac{\cos(x)}{x}dx$.

IV. KERR-LIKE BLACK HOLE METRIC IN DARK MATTER HALO

In Sec. III, we obtained the Schwarzschild-like black hole solutions in dark matter halos. Here, we use the NJ algorithm to generalize them to the rotation black hole case. Regarding the NJ algorithm, a lot of research and applications have been done [35–39].

For the first step of the NJ algorithm, it needs to transform the Schwarzschild-like black hole (3) to advanced null coordinates (u,r,θ,ϕ) by the following relation:

$$du=dt-\frac{1}{f(r)g(r)}dr. \tag{19}$$

Under the null tetrad, the inverse metric can be written as

$$g^{\mu\nu}=-l^\mu n^\nu-l^\nu n^\mu+m^\mu\overline{m}^\nu+m^\nu\overline{m}^\mu, \tag{20}$$

with l^μ, n^μ, m^μ, and $\overline{m}^\mu$ being

$$\begin{aligned}l^\mu&=\delta^\mu_r,\\n^\mu&=\sqrt{\frac{f(r)}{g(r)}}\delta^\mu_\mu-\frac{f(r)}{2}\delta^\mu_r,\\m^\mu&=\frac{1}{\sqrt{2}r}\delta^\mu_\theta+\frac{i}{\sqrt{2}r\sin\theta}\delta^\mu_\phi,\\\bar{m}^\mu&=\frac{1}{\sqrt{2}r}\delta^\mu_\theta-\frac{i}{\sqrt{2}r\sin\theta}\delta^\mu_\phi.\end{aligned} \tag{21}$$

In the null tetrad, these null vectors satisfy $l_\mu l^\mu=n_\mu n^\mu=m_\mu m^\mu=0$, $l_\mu n^\mu=-m_\mu\overline{m}^\mu=1$, and $l_\mu m^\mu=n_\mu m^\mu=0$. Next, we make a complex transformation,

$$\begin{aligned}u&\to u-ia\cos\theta,\\r&\to r+ia\cos\theta;\end{aligned} \tag{22}$$

then, we assume that these metric coefficients $f(r)$, $g(r)$, and $h(r)(=r^2)$ can be transformed to $F(r,\theta,a)$, $G(r,\theta,a)$, and $\Psi(r,\theta,a)$. In the new coordinate system, the null tetrad can be written as

$$\begin{aligned}l^\mu&=\delta^\mu_r,\\n^\mu&=\sqrt{\frac{G}{F}}\delta^\mu_\mu-\frac{F}{2}\delta^\mu_r,\\m^\mu&=\frac{1}{\sqrt{2\Psi}}\left(\delta^\mu_\theta+ia\sin\theta(\delta^\mu_\mu-\delta^\mu_r)+\frac{i}{\sin\theta}\delta^\mu_\phi\right),\\\bar{m}^\mu&=\frac{1}{\sqrt{2\Psi}}\left(\delta^\mu_\theta-ia\sin\theta(\delta^\mu_\mu-\delta^\mu_r)-\frac{i}{\sin\theta}\delta^\mu_\phi\right).\end{aligned} \tag{23}$$

Based on the transformed vectors (23), we obtain the nonzero components of metric tensor $g^{\mu\nu}$, and they are

$$g^{uu}=\frac{a^2\sin^2\theta}{\Psi},\qquad g^{\theta\theta}=\frac{1}{\Psi},$$
$$g^{ur}=g^{ru}=\sqrt{\frac{G}{F}}-\frac{a^2\sin^2\theta}{\Psi},$$
$$g^{\phi\phi}=\frac{1}{\Psi\sin^2\theta},\qquad g^{u\phi}=g^{\phi u}=\frac{a}{\Psi},$$
$$g^{r\phi}=g^{\phi r}=\frac{a}{\Psi},\qquad g^{rr}=G+\frac{a^2\sin^2\theta}{\Psi}. \tag{24}$$

Therefore, the Kerr-like black hole in Eddington-Finkelstein coordinates is

$$\begin{aligned}ds^2=&-Fdu^2+2\sqrt{\frac{F}{G}}dudr+2a\sin^2\theta\left(\sqrt{\frac{F}{G}}+F\right)dud\phi\\&-2a\sin^2\theta\sqrt{\frac{F}{G}}drd\phi+\Psi d\theta^2\\&-\sin^2\theta\left[-\Psi+a^2\sin^2\theta\left(2\sqrt{\frac{F}{G}}+F\right)\right]d\phi^2.\end{aligned} \tag{25}$$

If setting $k(r)=r^2\sqrt{f(r)}/\sqrt{g(r)}$, we can convert the Kerr-like black hole (25) to Boyer-Lindquist coordinates by the transformation

$$\begin{aligned}du&=dt-\frac{k+a^2}{r^2f(r)+a^2}dr,\\d\phi&=d\phi-\frac{a}{r^2f(r)+a^2}dr,\end{aligned} \tag{26}$$

and we choose

$$\begin{aligned}F(r,\theta)&=-\frac{r^2f(r)+a^2\cos^2\theta}{k(r)+a^2\cos^2\theta}\Psi,\\G(r,\theta)&=-\frac{r^2f(r)+a^2\cos^2\theta}{\Psi}.\end{aligned} \tag{27}$$

At the same time, we set $\Sigma^2=k(r)+a^2\cos^2\theta$, $2\bar{f}=k(r)-r^2f(r)$, $\Delta(r)=r^2f(r)+a^2$, and $A=(k(r)+a^2)^2-a^2\Delta\sin^2\theta$. We obtain the Kerr-like black hole metric

$$\begin{aligned}ds^2=&-\frac{\Psi}{\Sigma^2}\left(1-\frac{2\bar{f}}{\Sigma^2}\right)dt^2+\frac{\Psi}{\Delta}dr^2-\frac{4a\bar{f}\sin^2\theta\Psi}{\Sigma^4}dtd\phi\\&+\Psi d\theta^2+\frac{\Psi A\sin^2\theta}{\Sigma^4}d\phi^2.\end{aligned} \tag{28}$$

According to Refs. [36,38], because the metric (28) is rotational symmetric, $G_{r\theta}=0$. On the other hand, the metric (28) should satisfy Einstein's field equation $G_{\mu\nu}=8\pi T_{\mu\nu}$. For black hole metric (28), these conditions reduce to

$$(k+a^2y^2)^2(3\Psi_{,r}\Psi_{,y^2}-2\Psi\Psi_{,ry^2})=3a^2k_{,r}\Psi^2, \tag{29}$$

and

$$\begin{aligned}&\Psi[k_{,r}^2+k(2-k_{,rr})-a^2y^2(2+k_{,rr})]\\&\quad+(k+a^2y^2)(4y^2\Psi_{,y^2}-k_{,r}\Psi_{,r})=0,\end{aligned} \tag{30}$$

where $y=\cos\theta$, $\Psi_{,ry^2}=\partial^2\Psi/\partial r\partial y^2$, and $k_{,r}=\partial k(r)/\partial r$. For the rotation black hole surrounded by a CDM halo and BEC DM halo, the function $k(r)=r^2\sqrt{f(r)}/\sqrt{g(r)}$ is so complicated that Eqs. (29) and (30) have no analytic solution. From Sec. III, we know that our black hole solutions satisfy asymptotic conditions. Under the asymptotic conditions, the metric coefficients approximately satisfy $f(r)\approx g(r)$; therefore, $k(r)\approx r^2$. Combining Eqs. (29) and (30), we obtain $\Psi=r^2+a^2y^2$. Another reason why the above approximation is valid is that perturbation conditions can be considered when there is very little DM in the vicinity of the black hole.

Under above approximation condition, for the CDM halo and BEC DM halo, we give an analytical expression,

$$\begin{aligned}ds^2=&-\frac{r^2g(r)+a^2\cos^2\theta}{\Sigma^2}dt^2+\frac{\Sigma^2}{r^2g(r)+a^2}dr^2\\&-\frac{2a\sin^2\theta(k(r)-r^2g(r))}{\Sigma^2}d\phi dt+\Sigma^2d\theta^2\\&+\Sigma^2\sin^2\theta\left[1+a^2\sin^2\theta\frac{2k(r)-r^2g(r)+a^2\cos^2\theta}{\Sigma^2}d\phi^2\right],\end{aligned} \tag{31}$$

where $\Sigma^2=k(r)+a^2\cos^2\theta$, $k(r)\approx r^2$ and $\Delta=r^2g(r)+a^2$. When we do not consider dark matter, the black hole metric will degenerate into a Kerr black hole. For the CDM halo and BEC DM halo, we can get specific expressions [we substitute the corresponding $f(r)$ and $g(r)$, Eqs. (13)–(18), into Eq. (31) to get the specific expressions]. These black hole solutions describe the interaction between the spinning black hole and the dark matter halo; therefore, they should have some implications for understanding how dark matter affects black holes.

V. BLACK HOLE PROPERTIES

We obtain black hole solutions in dark matter halos, which include Schwarzschild-like and Kerr-like situations. For an example, we deduce the black hole metrics in the CDM halo and the BEC DM halo. In these black hole metrics, the interaction between dark matter and black holes is considered. Therefore, by analyzing the nature of these black holes, we can understand how dark matter changes the nature of black holes. In the following, we analyze the black hole horizon structure, stationary limit surfaces, ergosphere, and singularity structure. Since the actual dark matter models only change the black holes very little, we will calculate these properties by choosing

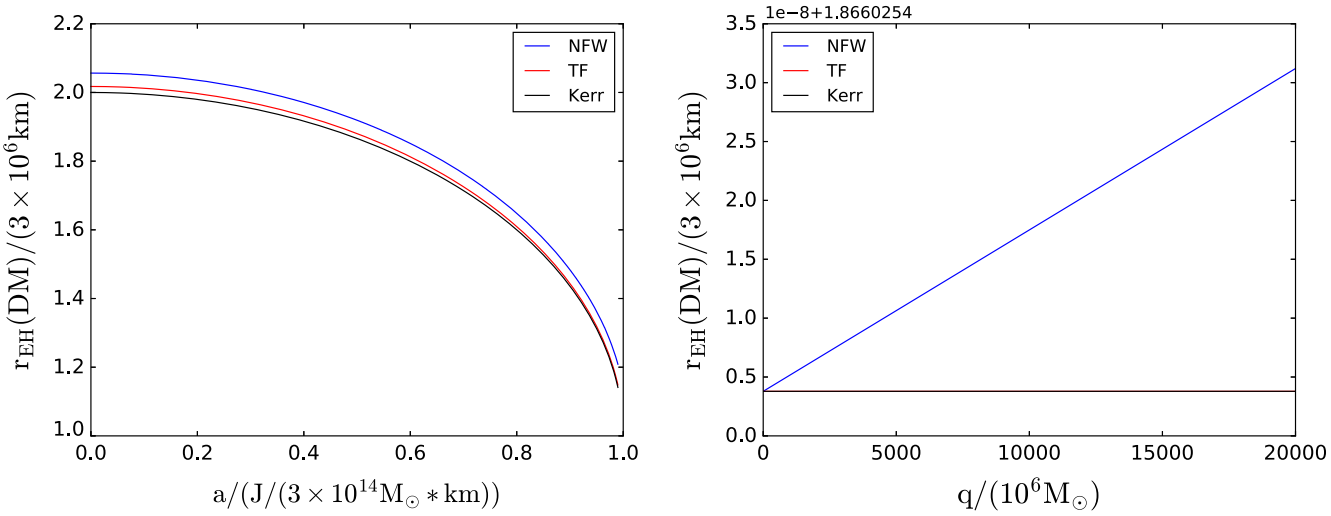

FIG. 1. The behavior of event horizon $r_{EH}(DM)$ with black hole spin a and dark matter parameter $q = \rho_s R_s^3$, where $q_{NFW} = 3.65 \times 10^{16}$ $M_\odot$, $R_s = 5.7 \times 10^{-4}$ Kpc, $q_{TF} = 3.4 \times 10^{21}$ $M_\odot$, $R = 2.92 \times 10^{-4}$ Kpc, and the black hole mass $M = 10^6$ $M_\odot$.

some toy parameters values (excluding Fig. 4). For the NFW profile, we choose $q_{NFW} = 3.65 \times 10^{16}$ $M_\odot$ and $R_s = 5.7 \times 10^{-4}$ Kpc [for the low surface brightness (LSB) galaxy ESO1200211, $q_{NFW} = 3.65 \times 10^8$ $M_\odot$, $M_{BH} = 1 \times 10^6$ $M_\odot$, $\rho_s = 2.45 \times 10^{-3}$ $M_\odot/pc^3$, and $R_s = 5.7$ Kpc] [40,41], where $M_\odot$ is the mass of the Sun. For the TF profile, we choose $q_{TF} = 3.4 \times 10^{21}$ $M_\odot$ and $R = 2.92 \times 10^{-4}$ Kpc (for the LSB galaxy ESO1200211, $q_{TF} = 3.4 \times 10^8$ $M_\odot$, $M_{BH} = 1 \times 10^6$ $M_\odot$, $\rho_s = 13.66 \times 10^{-3}$ $M_\odot/pc^3$, and $R = 2.92$ Kpc) [40,41]. To change the natural system of units to the international system of units, we replace $B(r) = 2M + K(r)$ with $\frac{G}{c^2}B(r) = \frac{2GM}{c^2} + \frac{GK(r)}{c^2}$, where c is the speed of light.

A. Event horizon

It is generally believed that the presence of a dark matter halo does not change the number of black hole horizons, like the Kerr black hole, which has two horizons, i.e., the Cauchy horizon $r_{EH}^-(DM)$ and event horizon $r_{EH}(DM)$. The nature of these horizons is precisely determined by the following equation: $\Delta = r^2 g(r) + a^2 = 0$. Specifically, for the CDM halo situation, the black hole horizon is described

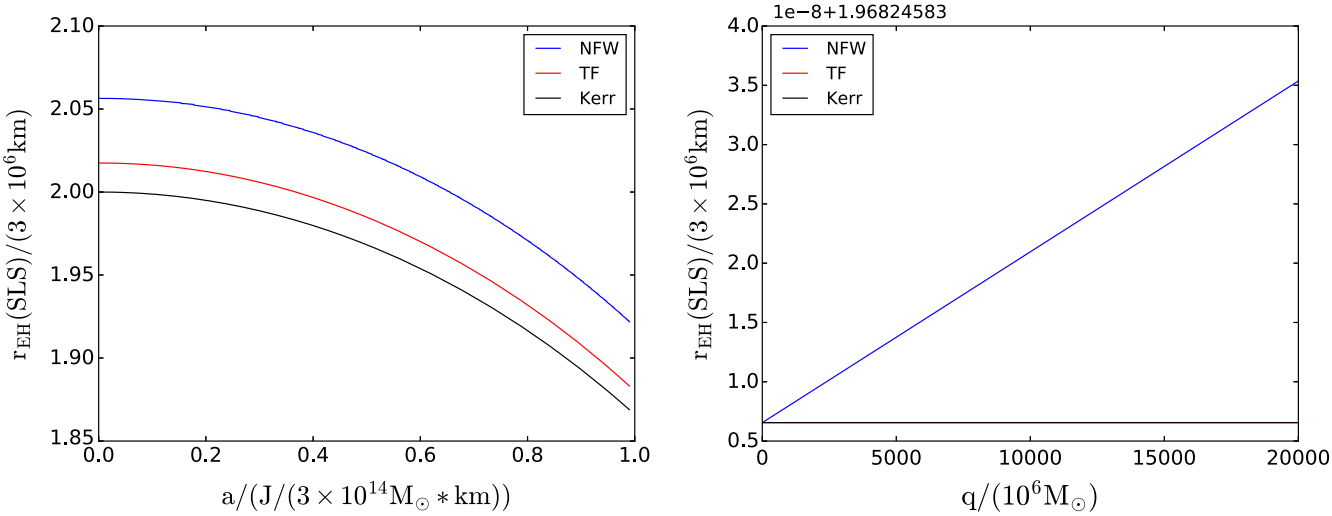

FIG. 2. The behavior of stationary limit surfaces $r_{SLS}(DM)$ with black hole spin a and dark matter parameters $q = \rho_s R_s^3$, where $\theta = \pi/3$, $q_{NFW} = 3.65 \times 10^{16}$ $M_\odot$, $R_s = 5.7 \times 10^{-4}$ Kpc, $q_{TF} = 3.4 \times 10^{21}$ $M_\odot$, $R = 2.92 \times 10^{-4}$ Kpc, and the black hole mass $M = 10^6$ $M_\odot$.

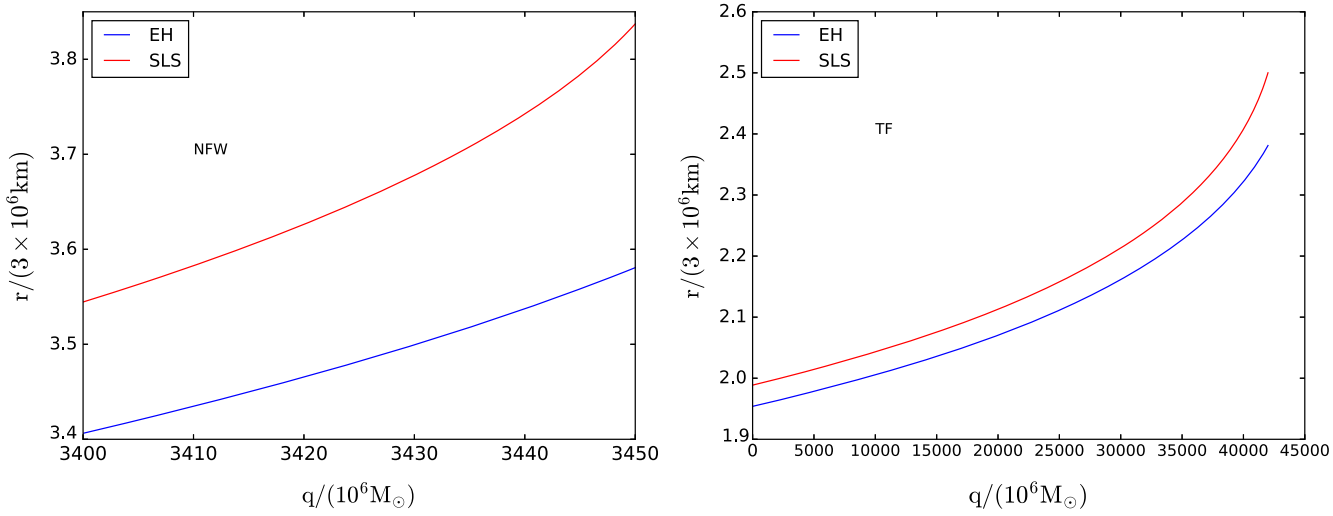

FIG. 3. The behavior of ergospheres scale $r = r_{\mathrm{SLS}}(\mathrm{DM}) - r_{+}(\mathrm{DM})$ with dark matter parameter $q = \rho_s R_s^3$, where $q_{\mathrm{NFW}} = 3.65\times10^{16}$ $\mathrm{M}_\odot$, $R_s = 5.7\times10^{-4}$ Kpc, $q_{\mathrm{TF}} = 3.4\times10^{21}$ $\mathrm{M}_\odot$, $R = 2.92\times10^{-4}$ Kpc, the black hole mass $M = 10^6$ $\mathrm{M}_\odot$, and $\theta = \pi/3$.

by the roots of the following equation: $r^2 - \frac{2GMr}{c^2} - \frac{8\pi G\rho_s R_s^3}{c^2}[r\ln(1+r/R_s) + rR_s/(r+R_s) - r] + a^2 = 0$. For the BEC DM halo situation, the equation becomes $r^2 - \frac{2GMr}{c^2} - 8G^2\rho_s R^3/(\pi^2c^2)\times[(\sin(\pi r/R) - \pi r/R\cos(\pi r/R)]r + a^2 = 0$. The behavior of the black hole horizon is determined by the black hole mass M, black hole spin a, dark matter characteristic density ρ_s, and scale radius R_s (or R). We obtain a schematic of the event horizon in Fig. 1, and we find that the dark matter halos increase the black hole horizon radius, and the CDM has a greater impact than the BEC DM. Qualitatively, these results (event horizon expansion for the black hole in the dark matter halo) is consistent with that in Ref. [31], but in this work, we generalize it to Kerr-like black hole situation.

B. Stationary limit surfaces

For Kerr-like black holes, the stationary limit surfaces are determined by g_{tt} of the metric, and they satisfy the condition $\Sigma^2 g_{tt} = r^2 - \frac{2MGr}{c^2} - \frac{GrK(r)}{c^2} + a^2\cos^2\theta = 0$. There are two roots in this equation, $r_{\mathrm{SLS}}^{-}(\mathrm{DM})$ and $r_{\mathrm{SLS}}(\mathrm{DM})$. Like the Kerr black hole case, these black holes also have an ergosphere area between $r_{\mathrm{EH}}(\mathrm{DM})$ and $r_{\mathrm{SLS}}(\mathrm{DM})$. In this area, there is a negative energy orbit. Because of the dark matter halo, dark matter makes the

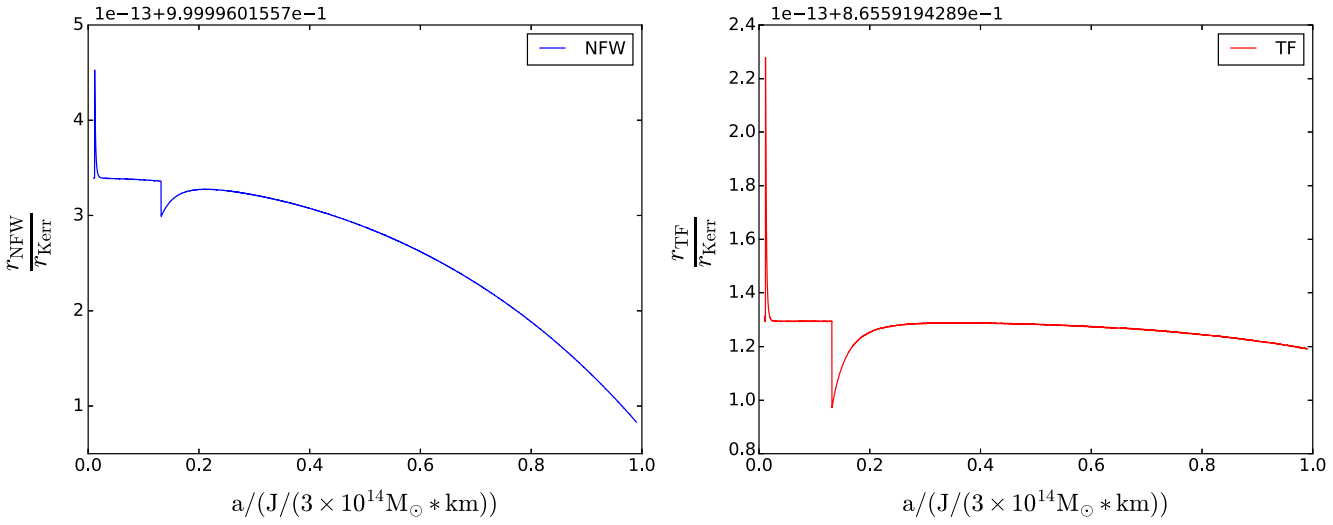

FIG. 4. The behavior of singularity ring radius $r(\mathrm{DM})/r_{\mathrm{Kerr}}$ with black hole spin a, where parameters $4\pi q_{\mathrm{NFW}}/R_s^2 = 1.37\times10^8$ $\mathrm{M}_\odot/\mathrm{pc}^2$ for NFW, $8\pi q_{\mathrm{TF}}/(3R^3) = 1.14\times10^{14}$ $\mathrm{M}_\odot/\mathrm{pc}^3$ for TF and $\omega = 0$. In this calculation, we only take a first-order approximation of function $B(r)$, and $\Phi(r)$ no longer takes asymptotic expansion.

black hole ergosphere have some new properties. For example, for the scale change of the stationary limit surface, the toy dark matter parameters are selected, and the stationary limit surface $r_{\mathrm{SLS}}(\mathrm{DM})$ increases (the results are shown in Fig. 2). The value is more than the increase in the black hole horizon; therefore, the dark matter halo enables the ergosphere area to increase (Fig. 3). Compared with the TF dark matter halo, the NFW dark matter halo shows a much larger ergosphere.

We know that energy can be extracted through the negative energy orbit of the ergosphere in a rotating black hole, which is the Penrose mechanism [42]. After that, the famous Blandford-Znajek mechanism was proposed [43], and it depends on the nature of the ergosphere. Our results show that a dark matter halo can increase the extracted energy.

C. Singularity structure

For a Kerr black hole, the singularity of the black hole is expressed as a ring, $r = 0$ and $\theta = \pi/2$. Therefore, a question about singularity would be the following: if the dark matter halo is considered around the black hole, how does the singularity of the black hole change? Through calculating the Kretsmann scalar $R = R^{\mu\nu\rho\delta}R_{\mu\nu\rho\delta}$, we find that the singularity of the black hole is determined by the equation $k(r) + a^2\cos^2\theta = 0$. Because $f(r) \neq g(r)$ and $k(r) \neq r^2$, the ring properties of black holes depend on dark matter halo parameters. This is very different from the Kerr black hole case. From Fig. 4, we find that the singularity ring radius decreases with increasing dark matter critical (center) density.

VI. SUMMARY

In this work, we obtained the solutions of a black hole immersed dark matter halos under asymptotic conditions and a constant equation of state. These black hole metrics include the Schwarzschild-like black hole and Kerr-like black hole. Then, we discussed how dark matter changes the nature of black holes, including the horizon structure, stationary limit surfaces, ergospheres, and singularity. We find that these properties are qualitatively different from the vacuum black hole solution. These may help us better understand the interaction between SMBHs and dark matter.

ACKNOWLEDGMENTS

Z. X. acknowledge the financial supported from the China Postdoctoral Science Foundation funded project under Grant No. 2019M650846. S.-N. Z. acknowledges supported by the National Program on Key Research and Development Project (Grant No. 2016YFA0400802) and National Natural Science Foundation of China under Grant No. U1838202.

[1] P. A. R. Ade *et al.* (Planck Collaboration), Astron. Astrophys. **594**, A13 (2016).
[2] G. Bertone and T. M. P. Tait, Nature (London) **562**, 51 (2018).
[3] J. S. Bullock and M. Boylan-Kolchin, Annu. Rev. Astron. Astrophys. **55**, 343 (2017).
[4] J. F. Navarro, C. S. Frenk, and S. D. M. White, Astrophys. J. **462**, 563 (1996).
[5] J. F. Navarro, C. S. Frenk, and S. D. M. White, Astrophys. J. **490**, 493 (1997).
[6] P. Bode, J. P. Ostriker, and N. Turok, Astrophys. J. **556**, 93 (2001).
[7] P. Colín, V. Avila-Reese, and O. Valenzuela, Astrophys. J. **542**, 622 (2000).
[8] D. N. Spergel and P. J. Steinhardt, Phys. Rev. Lett. **84**, 3760 (2000).
[9] W. Hu, R. Barkana, and A. Gruzinov, Phys. Rev. Lett. **85**, 1158 (2000).
[10] W. H. Press, B. S. Ryden, and D. N. Spergel, Phys. Rev. Lett. **64**, 1084 (1990).
[11] S.-J. Sin, Phys. Rev. D **50**, 3650 (1994).
[12] M. S. Turner, Phys. Rev. D **28**, 1243 (1983).
[13] K. G. Begeman, A. H. Broeils, and R. H. Sanders, Mon. Not. R. Astron. Soc. **249**, 523 (1991).
[14] L. Berezhiani and J. Khoury, Phys. Rev. D **92**, 103510 (2015).
[15] P. Gondolo and J. Silk, Phys. Rev. Lett. **83**, 1719 (1999).
[16] L. Sadeghian, F. Ferrer, and C. M. Will, Phys. Rev. D **88**, 063522 (2013).
[17] B. P. Abbott, R. Abbott, T. D. Abbott *et al.*, Phys. Rev. Lett. **116**, 131103 (2016).
[18] B. P. Abbott, R. Abbott, T. D. Abbott *et al.*, Phys. Rev. D **96**, 062002 (2017).
[19] D. E. Osterbrock, *Astrophysics of Gaseous Nebulae and Active Galactic Nuclei* (University Science Books, Mill Valley, CA, 1989), https://ui.adsabs.harvard.edu/abs/1989agna.book.....O/abstract.
[20] R. Antonucci, Annu. Rev. Astron. Astrophys. **31**, 473 (1993).
[21] S. Gillessen, P. M. Plewa, F. Eisenhauer *et al.*, Astrophys. J. **837**, 30 (2017).
[22] R. Abuter, A. Amorim *et al.* (Gravity Collaboration), Astron. Astrophys. **615**, L15 (2018).
[23] R. Abuter, A. Amorim, M. Bauboeck *et al.*, Astron. Astrophys. **625**, L10 (2019).
[24] K. Akiyama, A. Alberdi *et al.* (Event Horizon Telescope Collaboration), Astrophys. J. Lett. **875**, L1 (2019).

[25] F. D. Lora-Clavijo, M. Gracia-Linares, and F. S. Guzmán, Mon. Not. R. Astron. Soc. **443**, 2242 (2014).
[26] F. Munyaneza and P. L. Biermann, Astron. Astrophys. **436**, 805 (2005).
[27] M. Volonteri and M. J. Rees, Astrophys. J. **633**, 624 (2005).
[28] M. I. Zelnikov and E. A. Vasiliev, Int. J. Mod. Phys. A **20**, 4217 (2005).
[29] M. Le Delliou, R. N. Henriksen, and J. D. MacMillan, Astron. Astrophys. **526**, A13 (2011).
[30] M. Le Delliou, R. N. Henriksen, and J. D. MacMillan, Astron. Astrophys. **522**, A28 (2010).
[31] Y. Liu and S. N. Zhang, Phys. Lett. B **679**, 88 (2009).
[32] Z. Xu, X. Hou, X. Gong, and J. Wang, J. Cosmol. Astropart. Phys. 09 (2018) 038.
[33] W. J. G. de Blok, Adv. Astron. **2010**, 1 (2010).
[34] C. G. Böhmer and T. Harko, J. Cosmol. Astropart. Phys. 06 (2007) 025.
[35] E. T. Newman and A. I. Janis, J. Math. Phys. (N.Y.) **6**, 915 (1965).
[36] M. Azreg-Aïnou, Phys. Rev. D **90**, 064041 (2014).
[37] M. Azreg-Aïnou, Phys. Lett. B **730**, 95 (2014).
[38] M. Azreg-Aïnou, Eur. Phys. J. C **74**, 2865 (2014).
[39] R. Shaikh, Phys. Rev. D **100**, 024028 (2019).
[40] V. H. Robles and T. Matos, Mon. Not. R. Astron. Soc. **422**, 282 (2012).
[41] L. M. Fernández-Hernández, M. A. Rodríguez-Meza, and T. Matos, J. Phys. Conf. Ser. **1010**, 012005 (2018).
[42] R. Penrose, Nuovo Cimento Riv. Ser. 1 (1969), https://ui.adsabs.harvard.edu/abs/1969NCimR...1..252P/abstract.
[43] R. D. Blandford and R. L. Znajek, Mon. Not. R. Astron. Soc. **179**, 433 (1977).